University of Dundee

A Nonlocal Elasto-Plastic Model for Structured Soils at Large Strains for the Particle Finite Element Method

Monforte, Lluís; Ciantia, Matteo; Carbonell, Josep Maria; Arroyo, Marcos; Gens, Antonio

A nonlocal elasto-plastic model for structured soils at large strains for the Particle Finite Element method

Lluís Monforte[1], Matteo O Ciantia[2], Josep Maria Carbonell[3], Marcos Arroyo[4] and Antonio Gens[4]*

[1] School of Civil Engineering and Geosciences, Newcastle University, Newcastle upon Tyne (UK)

[2] School of Science and Engineering, University of Dundee, Dundee (UK)

[3] Centre Internacional de Mètodes Numèrics en Enginyeria (CIMNE), Barcelona (SPAIN)

[4] Universitat Politècnica de Cataluna - BarcelonaTech, Barcelona
Carrer Jordi Girona s/n, 08034, Barcelona (SPAIN)
antonio.gens@upc.edu

Abstract This work presents a robust and mesh-independent implementation of an elasto-plastic constitutive model at large strains, appropriate for structured soils, into a Particle Finite Element code specially developed for geotechnical simulations. The constitutive response of structured soils is characterized by softening and, thus, leading to strain localization. Strain localization poses two numerical challenges: mesh dependence of the solution and computability of the solution. The former is mitigated by employing a non-local integral type regularization whereas an Implicit-Explicit integration scheme is used to enhance the computability. The good performance of these techniques is highlighted in the simulation of the cone penetration test in undrained conditions.

Keywords: PFEM, Structured soils, Nonlocal elasto-plasticity, Constitutive modeling.

1 Introduction

Several elasto-plastic constitutive models have been proposed incorporating structure; these models are suitable to describe the behavior of soft rocks, natural clays or even artificially cemented soils (Gens Nova, 1993; Rouainia & Muir Wood, 2000; Wheeler et al, 2003; Rios et al, 2006, Ciantia, 2018). Structure results in an enhanced brittleness of the response along compression-dominated paths. Therefore, adding this realistic feature to constitutive descriptions is beneficial for more accurate predictions of structural response.

The simulation of brittle materials is conductive to strain localization (Zienkiewicz et al, 1995), which poses two numerical challenges, namely mesh dependency of the solution (Galavi and Schweiger, 2010) and the computability of the solution (Oliver et al, 2008).

In the context of Finite Elements, strain localization is highly influenced by the mesh: the width of the shear band is typically related to the element size whereas its direction is sometimes controlled by preferential alignment of the elements. Therefore, as the mesh is further refined, the thickness of the shear band decreases and the energy dissipated in the shear band tends to zero.

This pathological mesh dependence may be mitigated using regularization techniques, which incorporate a length scale to the constitutive model thereby enforcing the width of the localized region. Among regularization techniques, the nonlocal integral type has the advantage of not changing the field equations, which in turn results in a quite straight-forward implementation (Galavi and Schweiger, 2010; Mánica et al, 2018). In this approach the constitutive model is evaluated replacing some variables with its nonlocal counterpart, which is a spatial average in a neighborhood. Therefore, the constitutive response of a Gauss point is influenced by all the other integration points within a neighborhood, the size of which is determined with a characteristic length. Importantly, numerical simulations show that by using this approach, the thickness of the shear band is related to this characteristic length (Mánica et al, 2018).

In this work, an elasto-plastic model for structured materials at large strains is first described. Special attention is paid to its robust and mesh-independent implementation into a Finite Element code. The performance of the model is shown in a number of elementary tests. Finally, a representative simulation, namely a Cone Penetration test in undrained conditions, is presented to showcase the reliability of the numerical approach.

2 Constitutive equations

The constitutive model has been formulated in the framework of large strains elasto-plasticity with a multiplicative decomposition of the deformation gradient into elastic and plastic parts (Simo and Hughes, 1998). This framework ensures that rigid body motion of the deformable body do not produce spurious stress variations (frame indifference) and also that energy is preserved since a hyper-elastic model is employed.

The constitutive model for structured materials is built around the Modified Cam Clay model. The yield surface is defined as:

$$f(\boldsymbol{\tau}', p_s, p_t, p_m) = \left(\frac{q}{M}\right)^2 + p^*(p^* - p_c^*) \tag{1}$$

where $q = \sqrt{3J_2}$ and J_2 is the second invariant of the effective Kirchoff stress tensor, $\boldsymbol{\tau}'$. M is the slope of the Critical state line in the $p' - q$ plane whereas:

$$p^* = p' + p_t \tag{2}$$

$$p_c^* = p_t + p_s + p_m \tag{3}$$

where $p' = tr(\boldsymbol{\tau}')/3$ is the first invariant of the Kirchoff stress tensor.
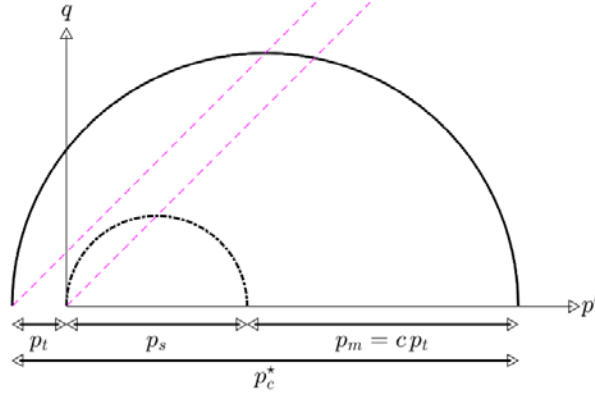
Fig. 1 Yield surface in the *p'-q* plane for axisymmetric compression

The yield locus in the triaxial plane is depicted in Figure 1; that also graphically defines the plastic stress-like variables p_c^*, p_t, p_s and p_m. On the one hand, p_s is the preconsolidation pressure of the reference, unstructured soil. On the other hand, p_t and p_m account for the effect of structure: p_m corresponds to the increase in the yield stress along isotropic compression paths whereas p_t is the tensile strength. Generally, these two hardening variables are considered to be proportional (Ciantia and di Prisco, 2016), being c the proportionality factor:

$$p_t = c \, p_m \tag{4}$$

The evolution of the hardening variables is related to the plastic volumetric and distortional flow:

$$\dot{p}_s = \rho_s \, p_s \left(\operatorname{tr}(\boldsymbol{l}^p) + \chi_s \sqrt{\frac{2}{3}} \, \|\operatorname{dev}(\boldsymbol{l}^p)\| \right) \tag{5}$$

$$\dot{p}_t = \rho_t \, p_t \left(|\operatorname{tr}(\boldsymbol{l}^p)| + \chi_s \sqrt{\frac{2}{3}} \, \|\operatorname{dev}(\boldsymbol{l}^p)\| \right) \tag{6}$$

where ρ_s, χ_s, ρ_t and χ_s are constitutive parameters and $\boldsymbol{l}^p$ is the spatial plastic velocity gradient.

The elastic response is characterized by means of an hyperelastic model incorporating a tensile range (Tamagnini et al, 2002), which is formulated in terms of the Hencky strain and the Kirchhoff stress tensor. Finally, associative plasticity is assumed.

This elasto-plastic model is integrated with an explicit stress integration technique (Monforte et al, 2014, 2019) based on Sloan et al (2001). The algorithm includes adaptive substepping and a yield surface drift correction algorithm.

An alternative stress integration technique is employed in this work, the so-called IMPLEX technique (Oliver et al, 2008). The strong nonlinearities of the constitutive model and strain localization may lead to numerical difficulties when an implicit time-marching scheme is used for the global problem: the numerical convergence rate may be seriously affected. The Finite Element stiffness matrix used in the Newton-Raphson scheme of the global problem may become so ill-conditioned that no convergence might be achieved even using very small time-steps (Alfano and Crisfield, 2001). The IMPLEX technique provides extra robustness and computability with respect to usual methods (Oliver et al, 2008). The interested reader is referred to Monforte et al (2019) for further details on the application of the IMPLEX technique to this constitutive model.

3   Nonlocal integration

A nonlocal integral type regularization technique is used to mitigate the pathological mesh-dependence that exhibit numerical simulations where softening is encountered. As such, the expression of a nonlocal variable $\tilde{\beta}$ is:

$$\tilde{\beta}(\boldsymbol{x}) = \frac{\int_\Omega w(\boldsymbol{x},\ \|\boldsymbol{x}-\boldsymbol{y}\|)\beta(\boldsymbol{y})\,d\Omega}{\int_\Omega w(\boldsymbol{x},\|\boldsymbol{x}-\boldsymbol{y}\|)\,d\Omega} \tag{7}$$

where $w(\boldsymbol{x},\ \|\boldsymbol{x}-\boldsymbol{y}\|)$ is the weighting function for point $\boldsymbol{x}$ controlling the influence of its neighbors in terms of their relative distance.

In this work, plastic strains are considered as nonlocal variables; from these values p_s and p_t may be obtained by integrating analytically Equations (5) and (6). The weighting function proposed by Galavi and Schweiger (2010) is employed here as it has been found to outperform other weighting functions in removing mesh bias.

4   Representative numerical simulations

The performance of the developed numerical model is demonstrated in a challenging numerical computation: the simulation of the cone penetration test in undrained conditions. The Particle Finite Element (Oñate et al, 2004) is used to tackle this large deformation problem. Further details on the numerical method may be found in Monforte et al (2017,2018).

The constitutive parameters have been chosen to represent a normally consolidated clay with a rigidity index of 150 (unstructured case). Three different cases have been considered with different level of structure: the initial value of p_t is changed from 0, 10 to 20 kPa. The values of the constitutive parameters are reported in Table 1. The initial stress state is characterized by $p' = 66.6$ kPa and $q = 50$ kPa, ($K_o = 0.5$).

Prior to analyze the response on the boundary value problem, Figure 2 reports the results of an anisotropically consolidated undrained triaxial (the effective stress path and the load-displacement curve). The case without structure exhibit the typical response of a Modified Cam Clay soil. On the other hand, the two cases in which structure is considered, first the material is loaded elastically until it reaches the yield surface; once the stress path reaches the yield surface, destructuration begins and deviatoric stresses decrease until the critical state is reached. The three cases have the same residual undrained shear strength. By increasing the degree of structure, the material becomes stronger and more brittle. Table 2 reports the peak and residual undrained shear strength.

Table 1 Constitutive parameter adopted in this work

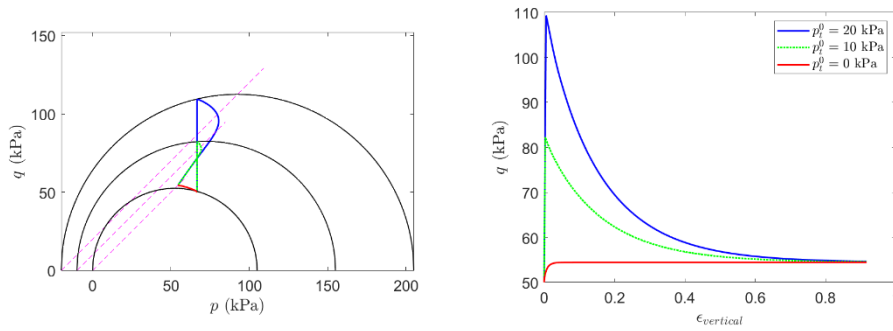| E	ν	M	p_s (kPa)	ρ_s	ρ_t	χ_s	χ_t	c	k (m/s)	K_0
8400	0.15	1	105	12	-12	0	0.5	5	10^{-12}	0.5

Fig. 2 Undrained triaxial response in the p-q plane (a) and evolution of deviatoric stresses in terms of the axial deformation. The cases are denoted by the amount of the initial structure. Subfigure (a) also depicts the initial yield surface.

Once the material has been characterized by means of the undrained triaxial, a CPTu in has been simulated. The cone of radius R=0.01784 m, is assumed rigid and smooth. The same initial stress state than in the triaxial tests has been assumed.

The net cone resistance and excess water pressure at the apex of the shaft and the cone (u_2 position) and in the midface of the cone (u_1 position) are reported in Figure 3. The mean value during penetration of the net cone resistance is 270 (kPa) for the case without structure and 321 and 359 kPa for the two cases with structure.

The cone factors (the net cone resistance divided by the undrained shear strength) are reported in Table 2; two different values have been calculated: one using the peak undrained shear strength, and another based on the residual. The shear strength corresponds to that of an anisotropically consolidated undrained triaxial test. For the case without structure the cone factor is around $N_{kt} = 9.9$, in good agreement with previous

numerical simulations. Meanwhile, the case with the most structure has a cone factor of 13.1 considering the residual strength and it drops to 6.6 if the peak strength is used to normalize the cone resistance.

Figure 3 also depicts the evolution of the excess water pressure at the u_1 and u_2 position. The water pressure is larger in the u_1 position with respect the u_2. The numerical results suggest that the excess water pressure increase with the brittleness of the soil.
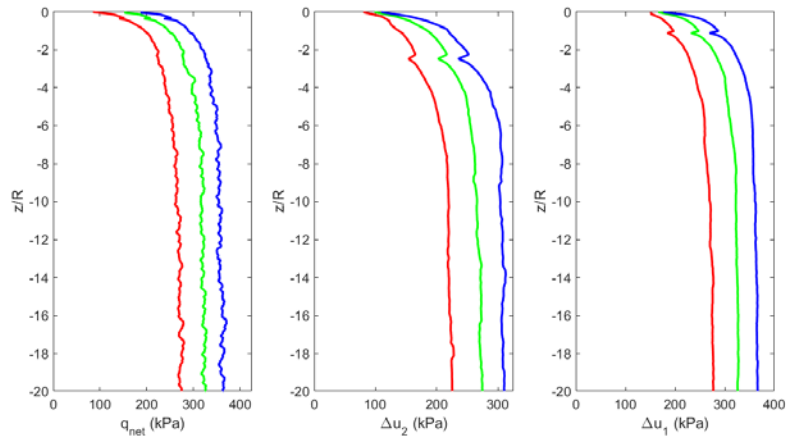

Fig.3 Evolution of the net cone resistance and excess water pressure at the u_2 and u_1 position in terms of the normalized penetration.
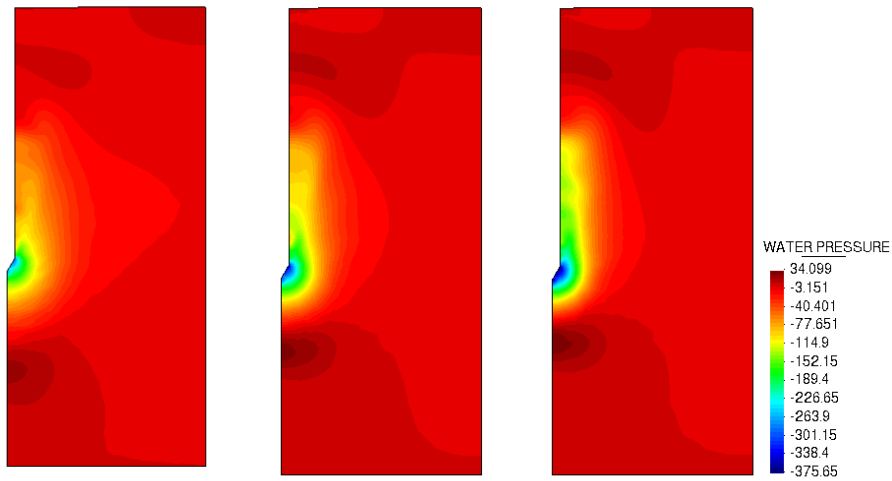

Fig.4 Excess water pressure after a penetration of $20R$ for the case unstructurated (left), $p_t = 10$kPa (middle) and $p_t = 20$ kPa (right).

Table 2 Cone factors and undrained shear strength (peak and residual) in terms of the initial value of p_t

p_t(kPa)	S_u^{peak} (kPa)	S_u^{res} (kPa)	$N_{kt}^{peak} = q_n/S_u^{peak}$	$N_{kt}^{res} = q_n/S_u^{res}$
0	27.5	27.5	9.8	9.8
10	41	27.5	7.8	11.7
20	54.5	27.5	6.6	13.1

Figure 4 reports the excess water pressure after a penetration of $20R$. In all the three cases, the maximum water pressure is found beneath of the cone, and high values of water pressure are also found close to the shaft of the tube. As more brittle materials are considered, larger excess water pressures are found.

5 Conclusions

This work has presented a large-strain elasto-plastic constitutive model for structured materials. The model has been reformulated employing a nonlocal integral type technique to avoid the pathological mesh-dependence that accompany strain localization whereas an IMPLEX integration scheme has been used to enhance the computability. The good performance has been demonstrated by the numerical simulation of the cone penetration test using the Particle Finite Element method.

References

Alfano, G. and Crisfield, M. A. (2001). Finite element interface models for the delamination analysis of laminated composites: mechanical and computational issues. International Journal for Numerical Methods in Engineering 50(7), 1701–36.

Ciantia M.O. and di Prisco C. (2016). Extension of plasticity theory to debonding, grain dissolution, and chemical damage of calcarenites. *International Journal for Numerical and Analytical Methods in Geomechanics* 40(3), 315–43.

Ciantia M.O. (2018) A constitutive model for the hydro-chemo-mechanical behaviour of chalk

Engineering in Chalk, 275-281

Galavi V. and Schweiger H.F. (2010). Nonlocal multilaminate model for strain softening analysis. *International Journal of Geomechanics* 10(1), 30–44

8

Gens, A. and Nova, R. (2009) Conceptual bases for a constitutive model for bonded soils and weak rocks. *Geomechanical Engineering of Hard Soils-Soft Rocks.*

Mánica, M.A., Gens, A., Vaunat, J. and Ruiz, D.F. (2018). Nonlocal plasticity modelling of strain localisation in stiff clays. *Computers and Geotechnics,* 103, 138–150.

Monforte, L, Arroyo, M., Carbonell, J.M. and Gens, A (2017) Insertion problems in geotechnical engineering with the Particle Finite Element method (PFEM), *Computers and Geotechnics,* 82, 144-156.

Monforte, L, Arroyo, M., Carbonell, J.M. and Gens, A (2018) Coupled effective stress analysis of insertion problems in geotechnics with the Particle Finite Element method, *Computers and Geotechnics,* 101, 114-129.

Monforte, L, Ciantia, M.O., Carbonell, J.M., Arroyo, M. and Gens, A (2019) A stable mesh-independent approach for numerical modelling of structured soils at large strains, *Computers and Geotechnics,* 101, 103215.

Oliver, J., Huespe, A.E. and Cante, J.C. (2008). An implicit/explicit integration scheme to increase computability of non-linear material and contact/friction problems. *Computer Methods Applied Mechanics and Engineering* 197(21), 1865–89.

Oñate, E., Idelsohn, S.R., del Pin, F. and Aubry, R. (2004) The particle finite element method – an overview. *International Journal of Computational Methods* 1(02), 267-307.

Rios, S., Ciantia, M., Gonzalez, N., Arroyo, M. and Viana da Fonseca, A. (2016). Simplifying calibration of bonded elasto-plastic models. *Computers and Geotechnics.* 73, 100–108.

Rouainia, M. and Muir Wood, D. (2000). A kinematic hardening constitutive model for natural clays with loss of structure. *Géotechnique* 50(2), 153–64.

Simo J.C. and Hughes T.J.R. (1998). *Computational inelasticity.* Springer Science & Business Media.

Sloan, S.W., Andrew, J.A. and Sheng, D. (2001) Refined explicit integration of elastoplastic models with automatic error control. Engineering Computations, 18(1/2), 121-194.

Tamagnini, C. and Castellanza, R. and Nova, R. (2002). A generalized backward Euler algorithm for the numerical integration of an isotropic hardening elastoplastic model for mechanical and chemical degradation of bonded geomaterials. *International Journal for Numerical and Analytical Methods in Geomechanics* 26(10), 963–1004

Wheeler, S.J., Näätänen, A., Karstunen, M. and Lojander, M. (2003). An anisotropic elastoplastic model for soft clays. *Canadian Geotechnical Journal* 40(2), 403–18.

Zienkiewicz, O.C., Huang, M. and Pastor, M. (1995) Localization problems in plasticity using finite elements with adaptive remeshing. *International Journal for Numerical and Analytical Methods in Geomechanics*, 19, 127–48.